Evidence for secondary-phase superconductivity in YNi4BC0.2'

Sullow, S.; Hendrikx, R.W.A.; Gortenmulder, T.; Nieuwenhuys, G.J.; Menovsky, A.A.; Schenk, A.; Mydosh, J.A.

Evidence for secondary-phase superconductivity in $YNi_4BC_{0.2}$

S. Süllow [a,*], R.W.A. Hendrikx [a], T.J. Gortenmulder [a], G.J. Nieuwenhuys [a],
A.A. Menovsky [a], A. Schenck [b], J.A. Mydosh [a]

[a] *Kamerlingh Onnes Laboratory, Leiden University, 2300 RA Leiden, The Netherlands*
[b] *Institute for Particle Physics, ETH Zürich, CH-5232 Villigen PSI, Switzerland*

Abstract

We have performed a metallurgical analysis of $YNi_4BC_{0.2}$ by X-ray diffraction and electron-probe microanalysis on as-cast and annealed samples. The superconducting properties of these samples were investigated by resistivity and μSR measurements. Our experiments indicate that $YNi_4BC_{0.2}$ is not superconducting as reported earlier, but that a second phase of the recently found quarternary compound YNi_2B_2C causes the zero resistance of $YNi_4BC_{0.2}$.

1. Introduction

Newly discovered intermetallic superconductors containing carbon have attracted much interest in the last half year due to their surprisingly high transition temperatures. Four different classes of superconductors have been found:

(1) $YPd_5B_3C_{0.3}$ shows superconductivity at 23 K, but the sample is inhomogeneous and the superconducting phase has not yet been identified [1],

(2) RT_2B_2C with R = Y, Lu, Ho, Er, Tm or Pr, T = Ni or Pt and T_c between 5 and 16.6 K [2,3],

(3) $ThPd_3B_2C$, an inhomogeneous system containing probably two superconducting phases of composition $ThPd_2B_2C$ ($T_c = 14.5$ K) and $ThPd_{0.65}B_{4.7}$ ($T_c = 21$ K) [4] and

(4) $YNi_4BC_{0.2}$ with $T_c = 12$ K [5].

The latter system is especially controversial regarding its superconducting properties. Previously Cava et al. [2] argued that superconductivity in

$YNi_4BC_{0.2}$ arises from a second phase, YNi_2B_2C. Hong et al. [6] arrived at the same conclusion. However, they examined $YNi_{4-x}B_{1+x}$ without specifically adding C and they did not directly prove that the superconductivity observable in their sample is due to the presence of YNi_2B_2C. In a similar claim of Felner [7] an unambiguous prove of second-phase superconductivity is also lacking.

In order to investigate the exact nature of the superconductivity in $YNi_4BC_{0.2}$, we directly studied its metallurgical and physical properties. Considerable data on the metallurgy have already been published [5,6,8,9]. YNi_4B crystallizes in the hexagonal CeCo$_4$B structure and lattice parameters are reported to be within 4.961 and 4.991 Å for the a-axis and 6.912 and 6.952 Å for the c-axis [6,8,10]. In addition a superstructure consisting of a three-fold a-axis was reported [11]. The crystallographic structure of as-cast $YNi_4BC_{0.2}$ is essentially the same as for YNi_4B. Only the superstructure seems to be absent in the carbonized sample [5]. Electron probe microanalysis (EPMA) has been performed on YNi_4B [6,8] as well as on $YNi_4BC_{0.2}$ [5], but in all cases the EPMA was

* Corresponding author. Fax: +31 71 275404; email: suellow@
rulgm0.LeidenUniv.nl.

only sensitive on Y and Ni, while B and C were undetectable. EPMA showed that all samples consisted of a matrix with a Y:Ni ratio of 1:4 with small inclusions of 1:2 and 1:5 ratio, respectively.

The physical properties of $YNi_4BC_{0.2}$ have been studied by bulk measurement techniques. Nagarajan et al. [5] concluded that adding C to YNi_4B generates superconductivity around 12 K by suppression of the crystallographic superstructure of pure YNi_4B. However, questions arose from the fact that the specific heat exhibited only a small anomaly at T_c and that the diamagnetic signal in the AC susceptibility experiment of a powdered sample gave only 10% of perfect diamagnetism at 5 K.

2. Metallurgy

Polycrystalline samples of $YNi_4BC_{0.2}$ have been arc-melted in stoichiometric ratio (Y:3N, Ni:4N, B:3N and C:3N) under argon atmosphere in a water-cooled copper crucible. The samples have been remelted seven times and the ingots were flipped over each time. The overall weight loss during the melting was about 0.2%. Parts of the samples have been annealed in evacuated quartz-tubes at 800°C for 2 and 5 days, respectively. One as-cast sample (referred to as S1) and one sample from the same batch, but annealed at 800°C for 2 days (S2), have been examined exhaustively by X-ray diffraction and EPMA. Our EPMA is sensitive to boron, whereas we can only detect carbon directly in the given phase for amounts higher than about 10 at.%. Two other samples from another batch, but produced in the same way, have been checked, one by X-ray diffraction (as-cast sample

S3); one by EPMA with only qualitative carbon analysis (at 800°C for 5 days annealed sample S4).

The results of the metallurgical analysis are summarized in Table 1. Annealed and as-cast $YNi_4BC_{0.2}$ show the presence of a minority phase in a matrix of YNi_4B stoichiometry. The different phases can be seen on the electron-backscattering photo (Fig. 1) of sample S1 as light gray regions (matrix) and dark regions (minority phase). The minority phase is itself inhomogeneous on a quite small scale (down to below 1 μm); the different grades of darkness in these regions indicate different local compositions. A similar morphology was observed for the samples S2 and

Fig. 1. Electron-backscattering photo of a polished surface of as-cast $YNi_4BC_{0.2}$, sample S1. Note the dark minority phase being itself inhomogeneous on a scale of smaller than 1 μm. The white spots to be seen at the photo are grains of the paste used to polish the surface of the sample.

Table 1
Composition and lattice parameters of $YNi_4BC_{0.2}$

	Phase	Y	Ni	B	C	a (Å)	b (Å)	c (Å)	I/I_0
S1	Matrix	1	3.9	0.9	≤10 at.%	4.983	4.983	6.945	1
	2	1	1.0	0.0	1.3	3.583	4.528	6.018	0.02
	3	1	13.3	4.1	≈10 at.%	9.609	7.376	10.98	0.03
	4	1	1.9	1.0	1.7	3.543	3.543	10.56	0.11
S2	Matrix	1	3.8	1.0	≤10 at.%	4.983	4.983	6.946	1
	2	1	1.2	0.0	2.3	3.573	4.509	6.020	0.12
	3	1	11.0	3.5	≤10 at.%	9.613	7.373	10.99	0.02
	4	1	1.2	0.6	1.7	3.546	3.546	10.74	0.11
S4	Matrix	1	4.0	1.1	≤10 at.%	–	–	–	–
	2	1	0.9	0.1	≥10 at.%	–	–	–	–
	3	1	2.0	1.8	≥10 at.%	–	–	–	–

S4. The volume amount of the minority phase has been estimated to be about 20%, but we were not able to distinguish between different phases in the minority phase, because the areas were too small to give a reliable estimate.

The compositions determined via EPMA, and given in Table 1, have been acquired with a standard procedure not fully suited for analyzing small regions. The results are not in all cases close to compositions of known intermetallic compounds. Especially for the minority phases two reasons can be mentioned:

(1) The extent of homogeneous secondary phase areas are of the order of or smaller than the spatial resolution of the microprobe (1 μm). Therefore, although the EPMA data clearly show trends of the local composition, the absolute values have to be taken with caution. This problem has been studied in more detail (see below).

(2) Further the secondary phases do not solidify under equilibrium conditions and especially boron and carbon have a tendency to be substituted interstitially in the host matrix. Consequently, it is likely that the phases present in our samples deviate from the compositions of regular intermetallic compounds.

With a higher resolution procedure we examined locally the distribution of Y, Ni and B in the inclusions in the YNi$_4$B matrix for the samples S1 and S2. In this analysis we observed a peculiar morphology of the phases given in Table 1. Following the notation of in Table 1 we found the phases 2 and 3 forming the central part of the inclusions. Phase 4 forms a thin layer around the center with a layer thickness of about 0.1–0.5 μm. Because of this small thickness we can not give the composition of phase 4 with high accuracy, since the other phases will influence the result.

Nevertheless we note that phase 4 is really a separate phase. Although the diameter of the electron beam restricts accurate quantitative analysis on areas larger than 1 μm, differences in local composition can qualitatively be observed in electron backscattering mode down to 0.1 μm, and in electron-backscattering examination phase 4 clearly shows up. Hence, the measured compositions of this phase give at least a rough estimate of the true composition. For sample S1 the measured compositions of Y:Ni:B are ranging from 1:2.5:0.7 to 1:1.8:1. For sample S2 the compositions are lying between 1:0.7:0.5 and

1:3:1.2. Furthermore we have to take into account the large carbon signal we observed for phase 4 and the presence of a phase YNi$_2$B$_{1.8}$C$_x$ in the sample S4. Thus, we argue that phase 4 is related to the quaternary compound YNi$_2$B$_2$C. We remark that this assumption could also explain the zero resistance observed for YNi$_4$BC$_{0.2}$, since the thin layers of phase 4 are quite likely to form a continuous zero-resistance path in the samples.

Our assumption can be tested by X-ray diffraction analysis. We took the secondary phases to be distorted derivatives of known compounds and fitted our X-ray data of the samples S1 and S2 as the sum of the spectra of the different phases. The EPMA data indicate the presence of four phases: hexagonal YNi$_4$B, orthorhombic YNiC$_2$, orthorhombic YNi$_{12}$B$_{6-x}$C$_x$ and tetragonal YNi$_2$B$_2$C [10,2]. By taking these phases into account we could quantitatively reproduce most of the peaks in our measured X-ray spectra with the lattice constants given in Table 1. Fig. 2 displays a typical X-ray diffraction pattern for S2. For sample S1 we can fit 46 of total 56 peaks, the highest intensity of a nonfitting peak being about 5%; for S2 we could fit 51 of total 60 peaks with about 3% highest intensity of misfitting peaks. As an estimate of the volume amount of the different phases we show in Table 1 the highest intensity I of fitting peaks of the appropriate structure normalized on the highest ab-
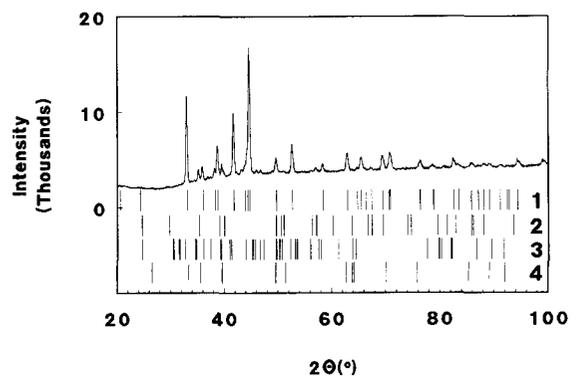

Fig. 2. X-ray spectrum of annealed YNi$_4$BC$_{0.2}$, sample S2. The ticks below the spectrum give the position of the Bragg reflections for the identified phases 1: (YNi$_4$B), 2: (YNiC$_2$), 3: (YNi$_{12}$B$_6$) and 4: (YNi$_2$B$_2$C).

solute intensity I_0. In the samples S1 and S2 we found the 100% peak of YNi_2B_2C being the largest, respectively, the second largest peak in our spectra not belonging to the YNi_4B structure. Also this peak could not be fitted with the structures of $YNiC_2$ or $YNi_{12}B_{6-x}C_x$.

X-ray diffraction was additionally used to investigate the effect of C on the superstructure of YNi_4B, and we found, similar to that reported in Ref. [5], no superstructure peaks in any of our X-ray studied samples.

3. Experiments

For the resistivity measurement we used a standard four-point AC technique between 1.3 and 300 K. The μSR measurements have been performed at the μSR facility of the Paul Scherrer Institut (PSI) in Villigen, Switzerland.

In Fig. 3, we show the normalized resistance of nominal $YNi_4BC_{0.2}$ for the samples S1–S4. The as-cast samples S1 and S3 show a sharp resistance drop at about 9 K with a tail at the low-temperature side for S1 (see insert). Zero resistance is reached at ≈ 7 K for S1 and at about 8.5 K for S3. The presence of the tail for S1 and its absence for S3 is already an indication for influence of sample inhomogeneities on superconductivity in $YNi_4BC_{0.2}$.

Annealing affects the superconducting transitions
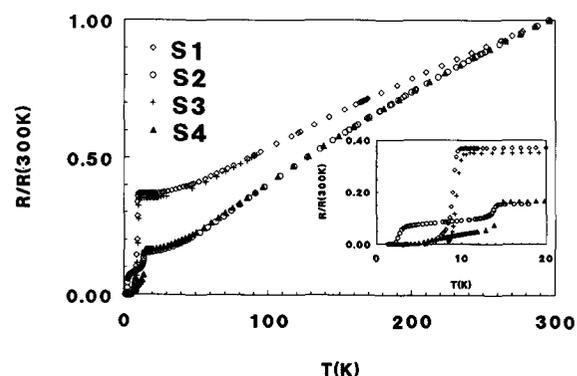

Fig. 3. Normalized resistance of $YNi_4BC_{0.2}$ as a function of temperature. The low-temperature range is shown in the insert. The resistivities at 300 K are 64 μΩ cm (S1), 66 μΩ cm (S2) and 50 μΩ cm (S4).

in an even more drastic way, as can be seen in Fig. 3. In both of our annealed samples the superconducting transition splits up into two transitions. The first transition temperature T_{c1} is situated at about 14–15 K with a resistance drop of $\approx 50\%$. The resistance goes finally to zero at $T_{c2} = 2.3$ K for S2 and 4.5 K for S4. By annealing, the second phases in $YNi_4BC_{0.2}$ are partly homogenized and crystallites of YNi_2B_2C are formed. Thus the sample undergoes a first superconducting transition close to T_c of YNi_2B_2C. However, only in parts of the second phase will YNi_2B_2C be formed. Other parts of the second phase will be driven away from the ideal 1221 composition, and therefore, a zero-resistance path will occur at lower temperatures than in the as-cast samples.

From our annealing experiments we can conclude that in annealed $YNi_4BC_{0.2}$ superconductivity arises from a second phase of YNi_2B_2C. But it might be possible that annealing only disintegrates the $YNi_4BC_{0.2}$ matrix into pure YNi_4B and free carbon. To prove that as-cast samples are not bulk superconductors we performed μSR experiments.

The μSR measurement was done on material from sample S1. μSR in a field probes superconductivity on a microscopic scale by detecting the internal field inhomogeneity due to the flux-line lattice of the superconductor. For the inverse relaxation rate t^{-1} in the superconducting state the relation holds [12]:

$$t^{-1} \propto \left[\lambda\sqrt{1 + \frac{16\pi^2\lambda^2}{3L^2}}\right]^{-1}, \qquad (1)$$

with λ the penetration depth and L the distance between the vortices. Therefore we measured the relaxation rate of $YNi_4BC_{0.2}$ in a transverse field of 0.035 T. The result is plotted in Fig. 4. Just below 9 K we see an increase of the inverse relaxation rate due to superconductivity. However, calculating from this increase the penetration depth we gain an extraordinary large value of λ with a lower boundary of $\approx 15\,000$ Å. Recently the penetration depth of YNi_2B_2C was determined to be 1500 Å [13]. Accordingly, the small increase of the inverse relaxation rate implies that most of the sample volume remains normal conducting. Hence, a more likely interpretation would be that the sample is not a bulk superconductor.
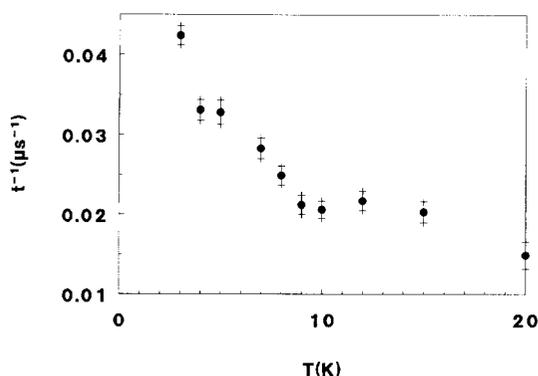
Fig. 4. Inverse muon relaxation rate of $YNi_4BC_{0.2}$, as-cast sample S1 in a transverse field of 0.035 T.

4. Conclusion

Our resistance measurements on annealed samples of $YNi_4BC_{0.2}$ show, compared to the as-cast material, a splitting of the superconducting transition with an increase of the first transition temperature T_{c1}. This increase of T_{c1} to 14–15 K can be explained assuming that the superconducting phase is YNi_2B_2C with a T_c of the bulk sample of 15.5 K. The initial T_c of as-cast $YNi_4BC_{0.2}$ is lower than that of YNi_2B_2C, since the superconducting second phase will be strongly distorted compared to the ideal structure. Annealing partly removes this distortion with a subsequent increase of T_{c1}. On the other hand the recrystallization of YNi_2B_2C breaks the former homogeneous low-resistance path and therefore the resistance drops to zero at a second $T_{c2} \leq T_c$ (as-cast).

From the μSR measurements on an as-cast sample of $YNi_4BC_{0.2}$ we have to draw the conclusion that the penetration depth calculated from these measurements is unusually large compared to typical already known superconductors or that the system is not a bulk superconductor. Taking also into account our metallurgical work we favor the second explanation. Further we can exclude in this way the possibility that annealing destroys the superconductivity of $YNi_4BC_{0.2}$ and produces the second-phase superconductor YNi_2B_2C. We remark that our observations

are in full agreement with the conclusions of Hong et al. [6] and Felner [7].

References

[1] R.J. Cava, H. Takagi, B. Batlogg, H.W. Zandbergen, J.J. Krajewski, W.F. Peck Jr., R.B. van Dover, R.J. Felder, T. Siegrist, K. Mizuhashi, J.O. Lee, H. Eisaki, S.A. Carter and S. Uchida, Nature (London) 367 (1994) 148.

[2] R.J. Cava, H. Takagi, H.W. Zandbergen, J.J. Krajewski, W.F. Peck Jr., T. Siegrist, B. Batlogg, R.B. van Dover, R.J. Felder, K. Mizuhashi, J.O. Lee, H. Eisaki and S. Uchida, Nature (London) 367 (1994) 252.

[3] R.J. Cava, B. Batlogg, T. Siegrist, J.J. Krajewski, W.F. Peck Jr., S. Carter, R.J. Felder, H. Takagi and R.B. van Dover, Phys. Rev. B 49 (1994) 12384.

[4] H.W. Zandbergen, T.J. Gortenmulder, J.L. Sarrac, J.C. Harrison, M.C. de Andrade, J. Hermann, S.H. Han, Z. Fisk, M.B. Maple and R.J. Cava, Physica C (#5860) •••.

[5] R. Nagarajan, C. Mazumdar, Z. Hossain, S.K. Dhar, K.V. Gopalakrishnan, L.C. Gupta, C. Godart, B.D. Padalia and R. Vijayaraghavan, Phys. Rev. Lett. 72 (1994) 274.

[6] N.M. Hong, H. Michor, M. Vyboronov, T. Holubar, P. Hundegger, W. Perthold, G. Hilscher and P. Rogl, Physica C 227 (1994) 85.

[7] I. Felner, Phys. Rev. Lett. 72 (1994) 3742.

[8] C. Mazumdar, R. Nagarajan, C. Godart, L.C. Gupta, M. Latroche, S.K. Dhar, C. Levy-Clement, B.D. Padalia and R. Vijayaraghavan, Solid State Commun. 87 (1993) 413.

[9] R. Nagarajan, C. Mazumdar, Z. Hossain, S.K. Dhar, K.V. Gopalakrishnan, L.C. Gupta, C. Godart, B. Padalia and R. Vijayaraghavan, Phys. Rev. Lett. 72 (1994) 3743.

[10] P. Villars and L.D. Calvert, Pearson's Handbook of Crystallographic Data for intermetallic Phases, 2nd. ed. (ASM, Ohio, 1989).

[11] Y.B. Kuz'ma and M.P. Khaburskaya, Izv. Akd. Nauk. SSSR Neorg. Matt. 11 (1975) 1893.

[12] A. Schenck, Muon Spin Rotation Spectroscopy (Adam Hilger, Bristol, 1985).

[13] M. Xu, P.C. Canfield, J.E. Ostenson, D.K. Finnemore, B.K. Cho, Z.R. Wang and D.C. Johnston, Physica C 227 (1994) 321.